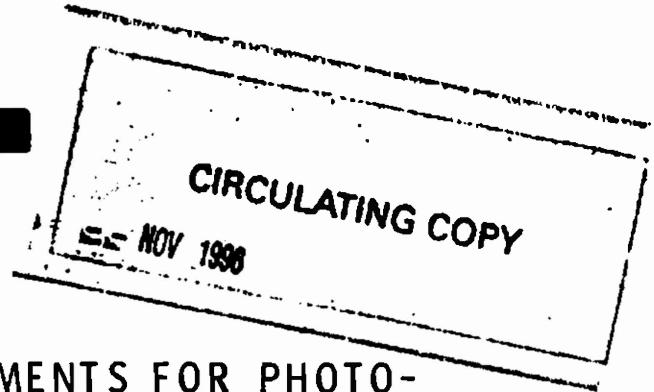# BRL

REPORT NO. 1922

CROSS SECTION MEASUREMENTS FOR PHOTO-
DETACHMENT OR PHOTODISSOCIATION OF IONS
PRODUCED IN GASEOUS MIXTURES OF O_2,
CO_2, AND H_2O

R. A. Beyer
J. A. Vanderhoff

September 1976

USA BALLISTIC RESEARCH LABORATORIES
ABERDEEN PROVING GROUND, MARYLAND

REPORT DOCUMENTATION PAGE		READ INSTRUCTIONS BEFORE COMPLETING FORM
1. REPORT NUMBER BRL REPORT NO. 1922	2. GOVT ACCESSION NO.	3. RECIPIENT'S CATALOG NUMBER
4. TITLE (and Subtitle) Cross Section Measurements for Photodetachment or Photodissociation of Ions Produced in Gaseous Mixtures of O_2, CO_2, and H_2O		5. TYPE OF REPORT & PERIOD COVERED BRL Report
		6. PERFORMING ORG. REPORT NUMBER
7. AUTHOR(s) R. A. Beyer* J. A. Vanderhoff		8. CONTRACT OR GRANT NUMBER(s)
9. PERFORMING ORGANIZATION NAME AND ADDRESS US Army Ballistic Research Laboratories Aberdeen Proving Ground, MD 21005		10. PROGRAM ELEMENT, PROJECT, TASK AREA & WORK UNIT NUMBERS RDT&E 1T161102B53A DNA S99QAXHD010
11. CONTROLLING OFFICE NAME AND ADDRESS USA Materiel Development & Readiness Command 5001 Eisenhower Avenue Alexandria, VA 22333		12. REPORT DATE SEPTEMBER 1976
		13. NUMBER OF PAGES 44
14. MONITORING AGENCY NAME & ADDRESS(If different from Controlling Office)		15. SECURITY CLASS. (of this report) Unclassified
		15a. DECLASSIFICATION/DOWNGRADING SCHEDULE

16. DISTRIBUTION STATEMENT (of this Report)

Approved for public release; distribution unlimited.

17. DISTRIBUTION STATEMENT (of the abstract entered in Block 20, if different from Report)

19. KEY WORDS (Continue on reverse side if necessary and identify by block number)
Photodetachment
Photodissociation
Negative Ions
Photon-Negative Ion Interaction
Drift Tube

20. ABSTRACT (Continue on reverse side if necessary and identify by block number)   srf
     A drift tube mass spectrometer coupled with a continuous laser photon source has been used to study photodissociation of thermal energy positive ion clusters. Absolute photodissociation cross sections have been measured for the singly charged positive ion of molecular oxygen clustered to one and two water molecules, clustered to molecular oxygen, and clustered to one carbon dioxide molecule. Upper limits have been established for the photodissociation cross sections of the atomic hydrogen positive ion clustered to one through four water molecules.   (see reverse side)

DD FORM 1473 EDITION OF 1 NOV 65 IS OBSOLETE
1 JAN 73

20. ABSTRACT: (Cont'd)

All of these measurements have been made at room temperature and for low field conditions (10 or 14.3 x 10 (-21) volt-square meter). Photon wavelengths ranging from 676.4 nm to 454.5 nm were studied.

The hydrated proton clusters were found to have small or zero cross sections. The single molecules of water and carbon dioxide clustered to the molecular oxygen cation have cross sections which behave similarly over part of the photon energy range. Near 2.60 eV both ions have cross sections approaching 6 x 10 (-22) square meter. The photodissociation of the molecular oxygen cation-carbon dioxide cluster produces a singly charged carbon dioxide cation photofragment. From the appearance of this fragment an upper bound on the dissociation energy of the molecular oxygen ion cluster to carbon dioxide was placed at 0.46 eV.

TABLE OF CONTENTS

.

This page Left Intentionally Blank

LIST OF TABLES

5

This page Left Intentionally Blank

LIST OF ILLUSTRATIONS

7

This page Left Intentionally Blank

I. INTRODUCTION

Recently it has been shown that weakly bound positive ion clusters can photodissociate at photon energies in the visible part of the spectrum. So far, experimental determination[1-4] of these cross sections is over a limited photon energy range and on only a handful of ion clusters, e.g., N_4^+, O_4^+, $O_2^+(H_2O)$, $H^+(H_2O)_{n=1-4}$, and some noble gas ions.[5] To expand this area we have extended our photodissociation cross section measurements to cover the energy range of $O_2^+(H_2O)$ in more detail and report here absolute photodissociation cross section measurements for $O_2^+(H_2O)_2$, $O_2^+(O_2)$, $O_2^+(CO_2)$, and $H^+(H_2O)_n$ at various discrete photon energies in the visible part of the spectrum.

These measurements have a direct application to the positive ion chemistry[6] of the D region of the atmosphere where the $H^+(H_2O)_n$ ions dominate the spectrum. Moreover, the $O_2^+(H_2O)$ and $O_2^+(O_2)$ provide possible path links for the conversion of O_2^+ to $H^+(H_2O)_n$. In addition to being a potentially important mechanism which must be considered in models of the ion chemistry of the daytime D region, information from photodissociation thresholds and photofragment ion appearances can be used to obtain bond energies and the location and shapes of bound and repulsive states for various species.

II. EXPERIMENTAL

A. Apparatus

The experimental apparatus consists of four major components: the ion source, the drift or thermalizing region, the mass spectrometer and ion detection electronics, and a continuous ion laser. A schematic representation of the apparatus is shown in Figure 1. Ions are formed

1 T. M. Miller, J. L. Heidrich, and J. T. Moseley, IX Int. Conf. on the Phys. of Electronic and Atomic Collisions, July 1975.

2 P. C. Cosby, Private Communication (1975).

3 J. A. Vanderhoff and R. A. Beyer, Chem Phys Lett 38, 532 (1976).

4 W. R. Henderson and A. L. Schmeltekopf, J. Chem. Phys. 57, 4502 (1972).

5 T. M. Miller, J. H. Ling, R. P. Saxon, and J. T. Moseley, Phys Rev, to be published.

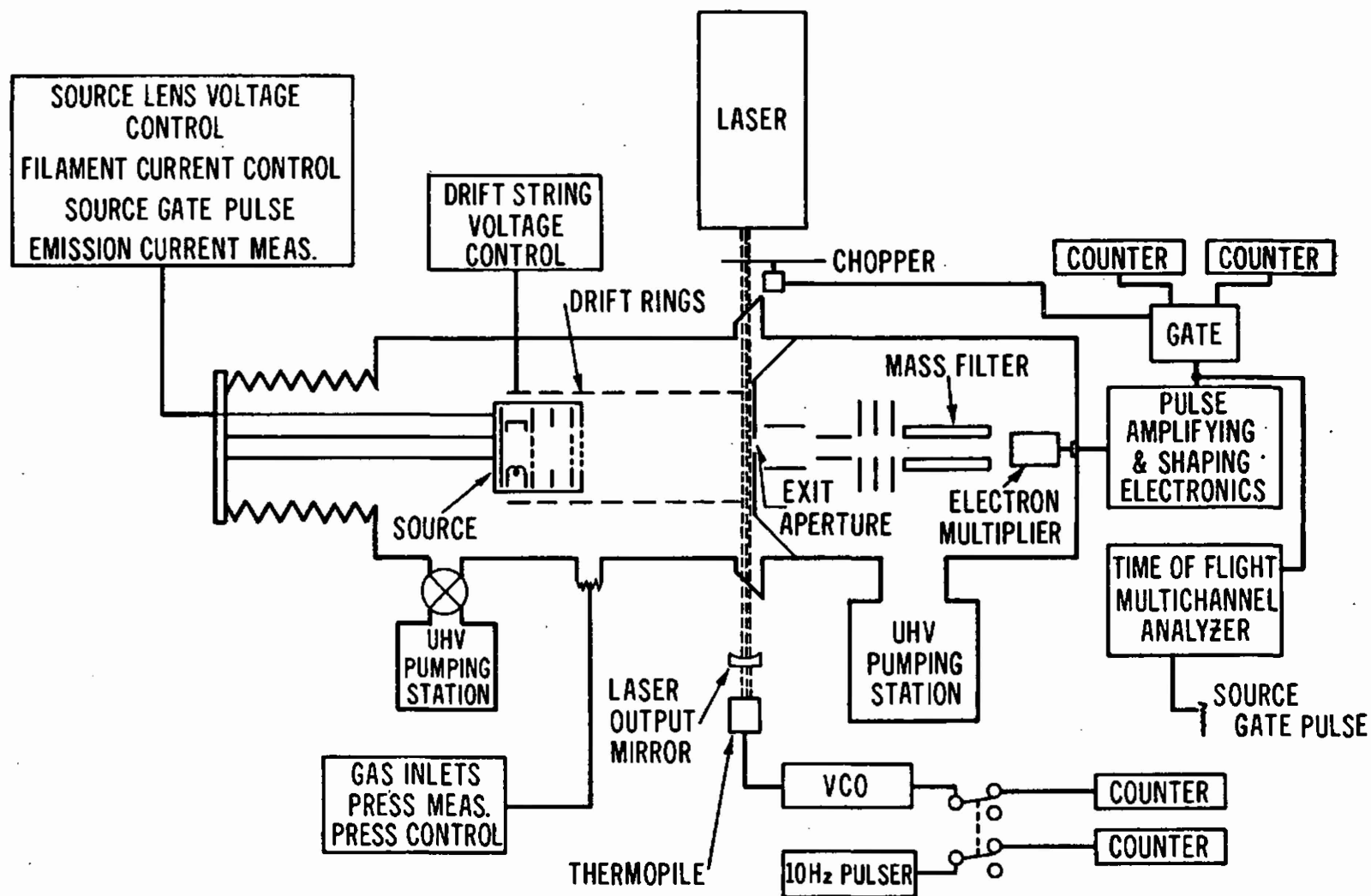6 E. E. Ferguson, Rev. Geophys. and Space Phys. 9, 93 (1972).

Figure 1. Schematic drawing of the experimental apparatus.

10

in the source from which they are extracted into the drift region. Under the influence of a weak uniform electric field, the ions drift toward the exit aperture while making many low energy collisions with the neutral gas molecules. During this drift time the ions diffuse and possibly react with the neutral species. Just in front of the exit aperture the ion swarm is intersected by a chopped laser photon source. The ions which pass through the exit aperture are accelerated to a mass filter, detected by an electron multiplier and the counts are gated to one of two counters depending on chopper position.

Negative ions are formed in the source by dissociative attachment or three body attachment of electrons to the neutral gas molecules. Positive ions are formed by ionization of the neutral gas by electron impact. Electrons emitted by a filament are accelerated transverse to the drift direction to a collector where the current is monitored. A small magnetic field ($\sim 7 \times 10^{-3}$ Wb/m^2) in the direction of electron travel assists in confining the electrons to the filament-collector region and increases the number of electron neutral collisions. Ions are extracted from this formation region through a hole of 12 mm diameter in the extractor plate. The remainder of the source consists of three lenses whose potentials may be adjusted to vary the ion residence time in the ion source region and thereby vary by up to an order of magnitude the relative concentrations of ions created by electron impact and those formed by subsequent ion-neutral reactions. The final lens is positioned in the midplane of a drift ring and is maintained at the potential of that ring. This arrangement provides a uniform drift field for the ions from the exit of the source to the sampling aperture. The last two lenses of the source can also be used to gate the ions. The resultant time arrival spectra can be used to extract ion mobilities and reaction rate coefficients.

The constant electric field drift region consists of eight evenly spaced stainless steel rings each of 102 mm diameter. The exit aperture of 1.0 mm diameter is centered in the midplane of the final, grounded drift ring. The potentials for the other seven drift rings are determined by an external voltage divider chain. The distance from the last source

11

lens to the exit aperture can be varied from 2 to 125 mm by moving the source. The source is mounted to the main vacuum chamber by a welded diaphragm stainless steel bellows to allow this movement to be made under vacuum conditions. Variation of the drift distance is used to adjust the relative concentrations of ions created or lost in ion-molecule reactions as well as allowing for relaxation of ions created in excited states. End effects which may be important in mobility measurements can be eliminated by obtaining data at two or more drift distances. One may also obtain ion-molecule reaction rate coefficients by variation of the drift distance.

Ions passing through the exit aperture enter a region of low pressure $\sim 10^{-3}$ N/m^2 (10^{-2} mTorr) as compared to 7 to 33 N/m^2 (50 to 240 mTorr) in the drift region. These ions are accelerated through collimating lenses to a potential of ~ 30 volts before they enter the mass filter which has better than 1 amu resolution. A channeltron multiplier and associated pulse counting electronics detect, amplify, and record this incoming signal.

The photon source is a continuous duty ion laser with a beam diameter of approximately 1.4 mm. Both argon and krypton laser tubes have been used. The discrete lines available with these laser tubes have an energy resolution of about 10^{-5} eV (1 eV = 1.602 x 10^{-19} J). Additionally, an argon ion laser has been used to pump a tunable dye laser to cover the wavelength region from 635 to 550 nm. The photon energy resolution of the dye laser was about 10^{-3} eV. Brewster windows on the drift tube and high reflectivity output mirrors were used to maximize intracavity light power. A thermopile was used to indicate the laser output power. To obtain the average power for a run, the thermopile output was converted to frequency and counted. This number along with a measurement of time for the run is used to calculate the average power. To convert this power into the actual intracavity power P_c the following relationship can be used

$$P_c(\lambda) = P_o(\lambda) \left[\frac{2-T(\lambda)}{T(\lambda)} \right] \tag{1}$$

12

where $T(\lambda)$ is the transmission of the laser output mirror and P_o is the output power. The intracavity laser power for these measurements ranged from 1 to 75 Watts. Only relative power measurements were necessary for the reduction of the data presented here. The laser beam is modulated with a 50 percent duty cycle by an intracavity 93 Hz chopper. This chopper also triggers a 32 MHz crystal controlled oscillator which produces equal width pulses for the gating of the ion counts to one of two counters alternately to give a measure of the ion count rate with light off and light on. As will be shown in the next section, the ratio of these two numbers, along with laser power and drift velocity values provide sufficient information to calculate photodestruction cross sections.

B. Analysis

The resultant intensity of an ion species subjected to a photon flux $\phi(\lambda)$ is given by

$$I(\lambda) = I_o e^{-B\sigma(\lambda)\phi(\lambda)t} \tag{2}$$

where I_o is the initial ion intensity, $\sigma(\lambda)$ is the cross section for the photon-ion interaction, t is the average time an ion spends in the photon beam, and B is a geometric term describing the overlap of the photon beam with the ion swarm which is sampled through the exit aperture. The photodestruction cross section can be written as

$$\sigma(\lambda) = \frac{B}{t\phi(\lambda)} \ln \frac{N_o}{N(\lambda)} \tag{3}$$

where $N(\lambda)$ and N_o are the counts detected at the particle multiplier with and without a flux of photons of wavelength λ, respectively. It is assumed that the ion intensity is proportional to these detected counts. For all data reported here the cross sections were measured relative to 0^-. Absolute values for the photodetachment cross section of 0^- at wavelengths of interest have been reported in the literature.[7]

[7] L. M. Branscomb, S. J. Smith, and G. Tisone, J. Chem. Phys. 43, 2906 (1965).

By making a relative measurement, experimental conditions can be fixed such that the value of B is not required; however, we did perform several initial checks by measuring the O^- photodetachment cross section.

Using six discrete lines of an argon ion laser (514.5 nm, 501.7 nm, 496.5 nm, 488.0 nm, 476.5 nm, and 457.9 nm) the photodetachment cross section for O^- was measured. The values obtained were consistent with previous published measurements[7] in that they were constant to within 10 percent. The largest contribution to this fluctuation arose from our inability to measure the small laser output mirror transmission for these wavelengths. To obtain the accepted value[7] of 6.3 x 10^{-22} m^2 for the photodetachment cross section of O^- a value for B near unity was required. This value was anticipated since the exit aperture and photon beam diameter are of similar size.

Normalization of the measured cross section to the O^- cross section eliminates the uncertainties associated with B and the absolute laser power. The photodestruction cross section of a positive or negative ion $A^{\pm}$ normalized to the O^- cross section can be written as

$$\sigma_{A^{\pm}}(\lambda) = \sigma_{0^-}(\lambda) \frac{\ln\left(\frac{No}{N(\lambda)}\right)_{A^{\pm}} P v_{A^{\pm}}}{\ln\left(\frac{No}{N(\lambda)}\right)_{0^-} v_{0^-}} \qquad (4)$$

where $\underline{P}$ is the ratio of laser powers $\left(\frac{P_{0^-}(\lambda)}{P_{A^{\pm}}(\lambda)}\right)$ for the $A^{\pm}$ and O^- cross

section measurements. Since the laser beam is not altered during the acquisition of the O^- and $A^{\pm}$ cross section data, the geometric term B does not change. The time an ion spends in the laser beam[2] has been replaced by the ion velocity. For the case where the ion makes a number of collisions while traversing the laser beam a drift velocity can be used for the ion velocity. Where possible drift velocities were obtained from published mobility data.

14

For other cases drift velocities were calculated from an expression given by Mason and McDaniel.[8] This equation for the low field drift velocity of an ion in a neutral gas is

$$v_d(0) = \frac{\xi}{3^{\frac{1}{2}}} \left(\frac{1}{m} + \frac{1}{M} \right)^{\frac{1}{2}} \frac{e}{(k_B T)^{\frac{1}{2}} Q} \left(\frac{E}{N} \right) \quad , \tag{5}$$

where m and M are the masses of the ion and the neutral, respectively. Q is the collision cross section and ξ is a factor of order unity. In order to mass scale the drift velocity or mobility, Eq. 5 is written as a ratio of two different species;

$$\frac{v_{d_1}(0)}{v_{d_2}(0)} = \frac{K_1(0)}{K_2(0)} = \frac{\left(\frac{1}{m_1} + \frac{1}{M_1} \right)^{\frac{1}{2}}}{\left(\frac{1}{m_2} + \frac{1}{M_2} \right)^{\frac{1}{2}}} \quad , \tag{6}$$

where $K_1(0)$ and $K_2(0)$ are the low field reduced mobilities of species 1 and 2, respectively. Here we have assumed that $\xi_1 = \xi_2$ and $Q_1 = Q_2$. Since both Q and ξ depend on the ion – neutral force laws this assumption should be reasonable for the comparison of ion – neutral systems with similar forces. However, anomalous effects from resonance charge transfer or large dipole moments cannot be characterized in this framework.

Some of the experimental data discussed in this report were obtained by use of gas mixtures. To compute the reduced mobility $K_{12}(0)$ of an ion in a gas mixture of fractional composition $x_1 + x_2$, Blanc's Law was used:

$$\frac{1}{K_{12}(0)} = \frac{x_1}{K_1(0)} + \frac{x_2}{K_2(0)} \quad . \tag{7}$$

Drift tube experiments usually report results as a function of the mean collision energy between the ions and the neutral gas. This energy

---

[8] E. W. McDaniel and E. A. Mason, *The Mobility and Diffusion of Ions in Gases*, (John Wiley and Sons, New York, 1973).

is expressed by the ratio of the applied drift field to the neutral gas density, E/N. The units for E/N are $V\text{-}m^2$ but are normally converted to Townsends (1 Townsend (Td) = 10^{-21} $V\text{-}m^2$). The cross section measurements reported here were made at an E/N of 10 or 14.3 Td. At these values the drift velocity for O^- is about an order of magnitude less than thermal velocity. Under these conditions, the molecular ions are thermalized while traversing the drift region.

III. RESULTS

A. O_2^- and CO_3^-

The photodetachment of O_2^- and the photodissociation of CO_3^- provide well documented cases of photodestruction of ions similar to those reported here. In this section we report on measurements of the cross sections for these processes. These values both confirm and extend those reported earlier.

Total photodestruction cross sections were measured for O_2^- formed in 13.3 N/m^2(100 mTorr) of research grade oxygen. Although the measured cross section for O_2^- at 514.5 nm was found to decrease above E/N values of 20 Td, the cross section was measured as constant within counting error at lower values, in agreement with Cosby et al.[9] The value of 10 Td was chosen for data acquisition as representative of thermal O_2^-. No variation was found in the O_2^- photodetachment cross section measured at 514.5 nm as a function of laser power, gas pressure, or drift distance.

From the results of other investigators, as well as the value of 4.1 eV[10] for the dissociation energy of O_2^-, the measured cross section may be assigned entirely to electron photodetachment. The present cross section measurements as a function of photon wavelength are shown as solid triangles in Figure 2 and listed in Table I. The photodetachment cross section for O_2^- has also been reported by Cosby et al.[9] Their ion laser results are shown as open triangles in Figure 2 and the values measured with a dye laser from 670 to 565 nm with a photon energy resolution of approximately 10^{-4} eV are represented by a solid line in

[9]P. C. Cosby, R. A. Bennett, J. R. Peterson, and J. T. Moseley, J. Chem. Phys., 63, 1612 (1975).
[10]P. H. Krupenie, J. Phys. Chem. Ref. Data, 1, 520 (1972).
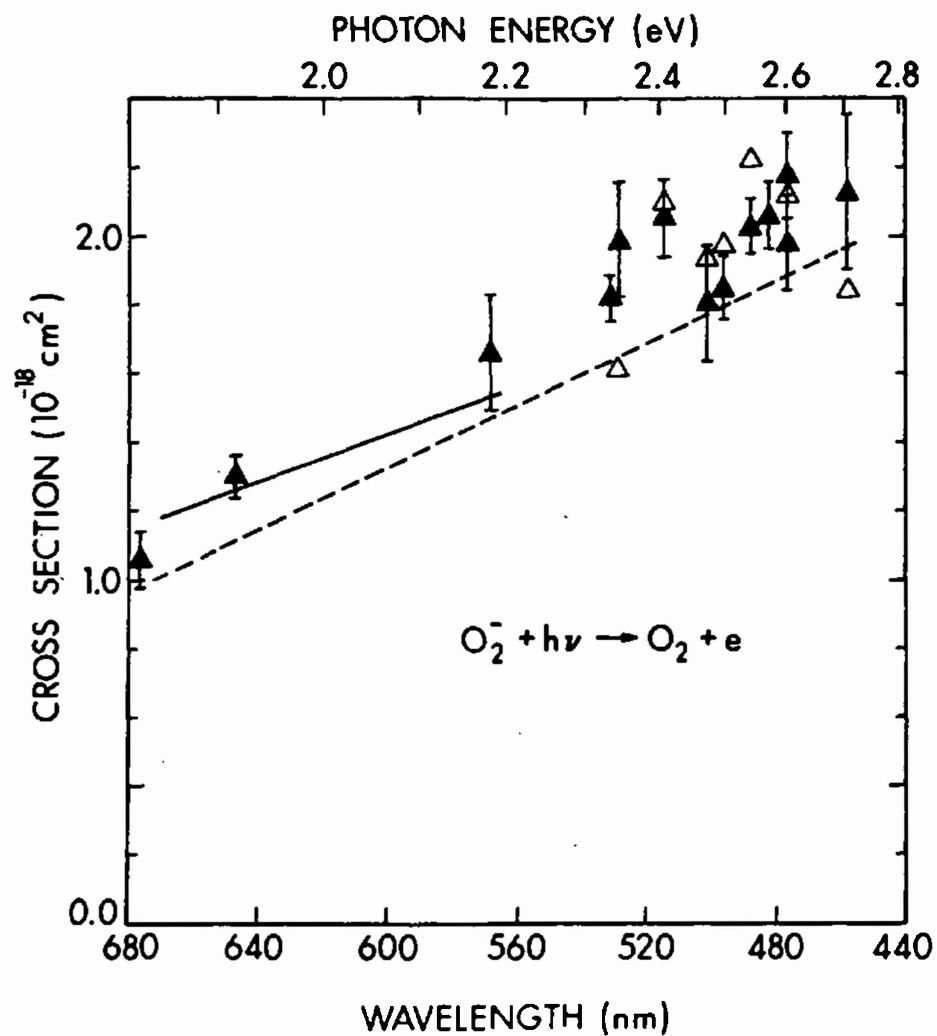
Figure 2. Photodetachment cross section versus photon energy for O_2^-.

The solid triangles are present results, the open triangles and the solid line represent the data of Cosby et al.[9] and the dashed line is an extrapolation of the data of Burch et al.[11]

Table I. Photodestruction Cross Section and Statistical Uncertainty Values for O_2^- and CO_3^- at an E/N = 10 Td.

Energy (eV)	$\sigma_{O_2^-}$ (10^{-22} m^2)	$\pm\Delta\sigma_{O_2^-}$ (10^{-22} m^2)	$\sigma_{CO_3^-}$ (10^{-22} m^2)	$\pm\Delta\sigma_{CO_3^-}$ (10^{-22} m^2)
1.833	1.06	0.08	0.09	0.04
1.916	1.30	0.06	0.98	0.05
2.182	1.66	0.17	1.34	0.33
2.335	1.82	0.07	1.01	0.11
2.345	1.99	0.17	--	--
2.410	2.06	0.12	0.75	0.08
2.471	1.80	0.17	0.80	0.20
2.497	1.85	0.10	0.53	0.10
2.540	2.03	0.08	0.45	0.06
2.569	2.06	0.10	0.49	0.13
2.602	2.18	0.13	0.77	0.11
2.603	1.98	0.14	0.93	0.18
2.707	2.13	0.23	0.88	0.31

the figure. Burch et al.[11] and Warneck[12] have also measured the O_2^- photodetachment cross section using beam techniques with a glow discharge ion source. The dashed line represents an extrapolation of the data of Burch et al. from 1.82 to 2.72 eV, measured with an energy resolution of about 0.2 eV. The data of Warneck are not shown but follow closely that of Burch et al. The much larger values of Burt[13], which have been questioned by Cosby et al. as being affected by O^- photofragments from photodissociation of O_3^- , are not shown.

The general agreement for the photodetachment measurements of O_2^- is quite good. The discrete argon ion wavelengths in the 2.35 to 2.71 eV energy range indicate that possibly more structure is present in the cross section than suggested by the low energy resolution data; however, a detailed investigation of this region would be required to demonstrate the existence of structure as opposed to a smoothly increasing cross section.

Photodissociation cross sections for CO_3^- have been reported[14,15] for various photon energies in the visible region. This documented photodissociation of a thermal energy molecular ion provides a test case for our system. Although previous measurements were made in pure CO_2 gas, the values reported here were measured in O_2-CO_2 gas mixtures. The total gas pressure used was 6.66 N/m^2 (50 mTorr) with 20 to 50 percent CO_2. With this mixture sufficient count rates of O^-, O_2^-, CO_3^-, as well as trace amounts of CO_4^- were obtained at an E/N of 10 Td. The pressure is maintained at this relatively low value to minimize error due to recombination of O^- photofragments with CO_2 since CO_3^- has been reported[14,15] to photodissociate into O^- and CO_2. With our laser beam-sampling orifice geometry one must increase the CO_2 pressure substantially

[11]D. S. Burch, S. J. Smith, and L. M. Branscomb, Phys. Rev. 112, 171 (1958).
[12]P. Warneck, GCA Technical Report 69-13-N, GCA Corporation, Bedford, MA, 1969.
[13]J. A. Burt, Can. J. Phys. 50, 2410 (1972).
[14]J. T. Moseley, R. A. Bennett, and J. R. Peterson, Chem. Phys. Lett. 26, 288 (1974).
[15]J. T. Moseley, P. C. Cosby, R. A. Bennett, and J. R. Peterson, J. Chem. Phys., 62, 4826 (1975).

above the value used before noticeable decreases in the apparent cross section are observed. To eliminate further possible error arising from an 0^- photofragment ion, the CO_3^- cross sections were normalized to our measured values for the O_2^- photodetachment cross section. Our measurements of the CO_4^- photodestruction cross section at 676.4 nm, 647.1 nm, and 514.5 nm indicate that its value is much less than the photodetachment cross section for O_2^-. Cosby[2] has measured the photodestruction cross section of CO_4^- in the wavelength region from 660 to 515 nm and finds values less than $2 \times 10^{-23} m^2$. This cross section together with the quantity of CO_4^- present in the ion spectrum makes possible errors due to CO_4^- photodissociation to O_2^- less than 0.3 percent.

To obtain the required drift velocities for O_2^- and CO_3^- drifting in the gas mixture the following procedure was used. Low field reduced mobilities for 0^- and CO_3^- drifting in CO_2 have been measured by Cosby[2] as $1.92 \times 10^{-4} m^2/V\text{-}s$ and $1.34 \times 10^{-4} m^2/V\text{-}s$, respectively. Snuggs et al.[16] have measured the reduced mobility of CO_3^- in O_2 as $2.50 \times 10^{-4} m^2/V\text{-}s$. As no published value for the mobility of O_2^- in CO_2 was available, this mobility was calculated by mass scaling the mobility of 0^- in carbon dioxide through use of Eq. 6. The resultant value obtained is $1.53 \times 10^{-4} m^2/V\text{-}s$. To obtain the required low field mobility for the gas mixture Eq. 7 was used.

The photodestruction cross section values measured are shown as solid circles in Figure 3 and listed in Table I. Photodestruction cross section values for CO_3^- reported by Moseley et al.[15] are also plotted on Figure 3. The open circles represent their data using an argon ion laser, and the half-solid circles represent data acquired using an argon ion laser pumped tunable dye laser. Burt[17] has reported larger photodetachment cross sections for CO_3^- in the energy range reported here; however, in addition to the question of the photodestruction mechanism[18,19], the

[16]R. M. Snuggs, D. J. Volz, J. H. Schummers, D. W. Martin, and E. W. McDaniel, Phys. Rev. A 3, 477 (1971).

[17]J. A. Burt, J. Chem. Phys. 57, 4649 (1972).

[18]E. E. Ferguson, F. C. Fehsenfeld, and A. V. Phelps, J. Chem. Phys. 59, 1565 (1973).

[19]J. A. Burt, J. Chem. Phys. 59, 1567 (1973).

PHOTON ENERGY (eV)
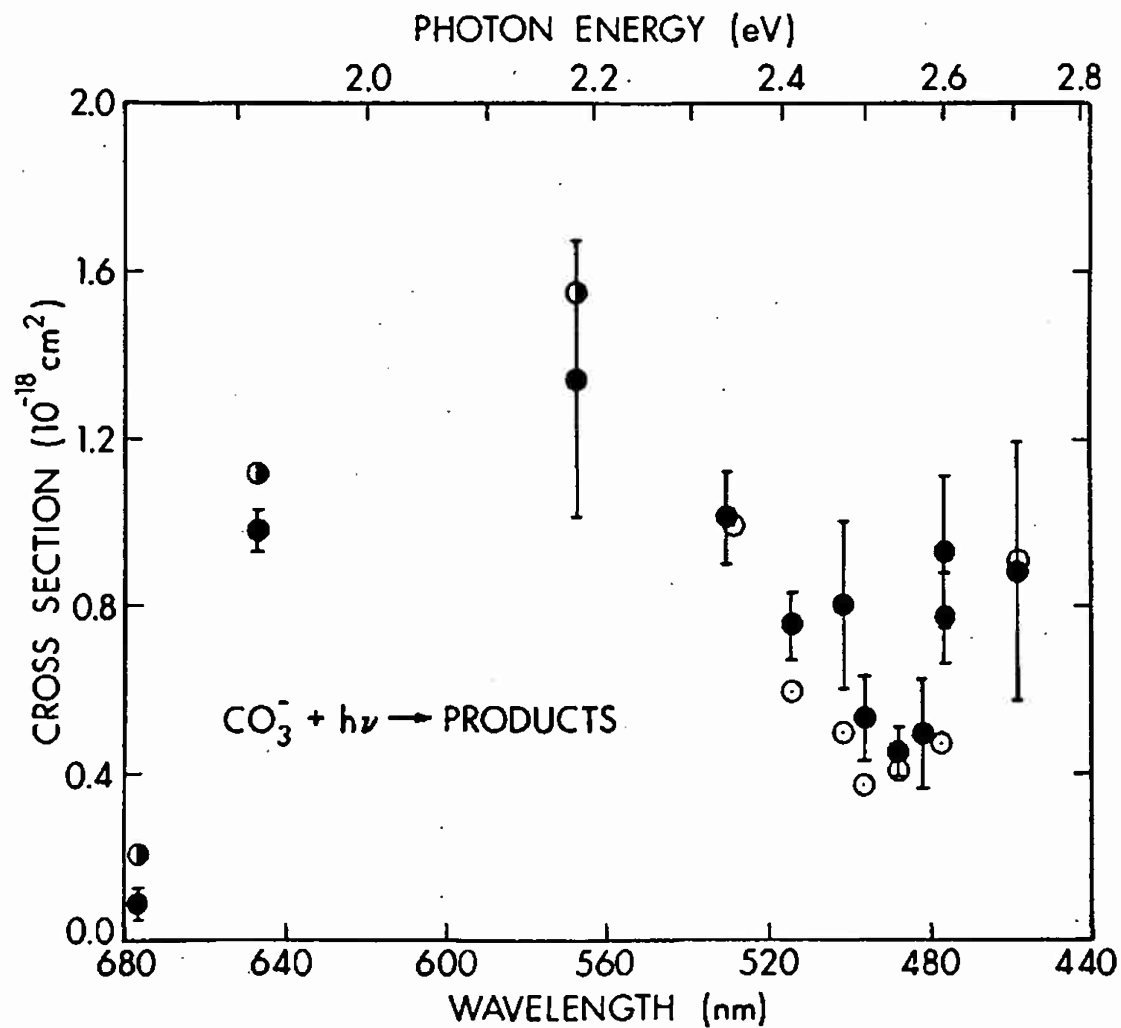
$CO_3^- + h\nu \rightarrow$ PRODUCTS

Figure 3.   Photodestruction cross section versus photon energy for CO_3^-.
The solid circles are present results.   The open circles and
half solid circles represent the data of Moseley et al.[14,15,21].

magnitudes of these cross sections have been questioned by recent experiments.[14,15] Under conditions where CO_3^- was the dominant ion, we have observed photoproduction of O^- at 514.5 nm consistent with the finding of Moseley et al.[14,15] that most, if not all, of the observed photodestruction cross section over the energy region of 1.85 to 2.71 eV is due to photodissociation. Very recently Hong et al.[20] have reported a photodetachment threshold for CO_3^- of 2.69 $\pm$ 0.1 eV.

The agreement between the two sets of data shown in Figure 3 is good and suggests that structure may be present. Cosby et al.[21] have used a tunable dye laser and obtained detailed structure over the region from 640 to 565 nm. They interpret this spectrum as resulting from vibrational structure of a bound predissociating state of CO_3^-. The overall agreement of our photodetachment and photodissociation measurements of O_2^- and CO_3^-, respectively, with those reported previously demonstrate the consistency of measurements made in this manner.

B. $O_2^+(H_2O)$ and $O_2^+(O_2)$

Photodissociation cross section measurements for the weakly bound positive cluster ions $O_2^+(H_2O)$ and $O_2^+(O_2)$ were made in 32.0 N/m^2 (240 mTorr) of research grade oxygen with trace amounts of water vapor added. The water vapor partial pressure was less than 0.13 N/m^2 (1 mTorr). The gas temperature was near room temperature, approximately 296K. This gas mixture produced sufficient amounts of $O_2^+(H_2O)$ and $O_2^+(O_2)$ for photo-dissociation measurements and also the amount of O^- necessary for normalization. All positive ion cross section measurements reported here were made at an E/N of 1.43 x 10^{-20}V-m^2 (14.3 Td). Approximately 20 volts potential difference between the filament and electron collector was sufficient to produce copious quantities of O_2^+. Subsequent relevant reactions are
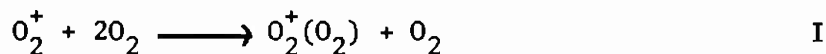
$$O_2^+ + 2O_2 \longrightarrow O_2^+(O_2) + O_2 \qquad\qquad I$$

[20]S. P. Hong, S. B. Woo and E. M. Helmy, Bull. Am. Phys. 21, 170 (1976).
[21]P. C. Cosby and J. T. Moseley, Phys. Rev. Letters 34, 1603 (1975).

followed by $\quad\quad O_2^+(O_2) + H_2O \longrightarrow O_2^+(H_2O) + O_2$ $\quad\quad\quad$ II

or $\quad\quad\quad O_2^+ + H_2O + O_2 \longrightarrow O_2^+(H_2O) + O_2$. $\quad\quad\quad$ III
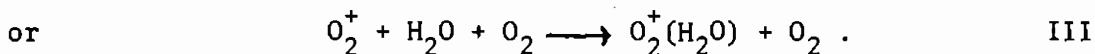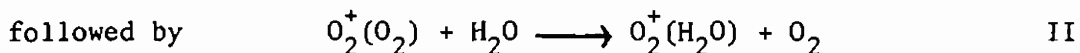
Considering the rate coefficients[22] and the gas densities, the dominant reaction path for the formation of $O_2^+(H_2O)$ in our experiment is I followed by II. The positive ion spectrum consisted of the above mentioned ions and trace amounts of the $H^+(H_2O)_{n = 1-4}$ series formed in $O_2 - H_2O$ mixtures. Small amounts of $O_2^+(H_2O)_2$ were also formed although the intensity was more than two orders of magnitude less than that of $O_2^+(H_2O)$. The photo-dissociation cross section of this ion has been measured to be comparable or less than the photodissociation of $O_2^+(H_2O)$ (see section D); consequently possible error due to photodissociation of $O_2^+(H_2O)_2$ into $O_2^+(H_2O)$ photo-fragments is entirely negligible for these experimental conditions.

These positive ion photodissociation cross sections were placed on an absolute scale by normalization to O^-. All experimental conditions were left the same except for the reversal of appropriate polarities and changing the potential difference of the filament to electron collector to about 8 volts. This provided sufficient amounts of O^- by dissociative attachment to O_2.

The observed photodissociation cross sections for $O_2^+(H_2O)$ and $O_2^+(O_2)$ as functions of photon energy are given in Table II and shown in Figures 4 and 5, respectively. We have previously reported[3] on the photodissociation cross sections of $O_2^+(H_2O)$; however, the present measurements include data over the wavelength range from 635 to 550 nm obtained with an argon ion laser pumped tunable dye laser. The error bars shown on the figures are a measure of the total relative error, which in many cases is dominated by counting error, as discussed in the error analysis section. These cross sections were computed from Eq. 4 using the values of Branscomb et al.[7] for the photodetachment of O^-. The drift velocities of O^- and $O_2^+(O_2)$ were obtained from the reduced mobility data of Snuggs et al.[16].

---

[22]C. J. Howard, V. M. Bierbaum, H. W. Rundle, and F. Kaufman, J. Chem. Phys. 57, 3491 (1972).

Table II. Photodissociation Cross Section and Statistical Uncertainty Values in Units of 10^{-22} m^2 for $O_2^+(H_2O)$, $O_2^+(H_2O)_2$, $O_2^+(O_2)$, and $O_2^+(CO_2)$ at an E/N = 14.3 Td

Energy	$O_2^+(H_2O)$		$O_2^+(H_2O)_2$		$O_2^+(O_2)$		$O_2^+(CO_2)$	
eV	σ	±Δσ	σ	±Δσ	σ	±Δσ	σ	±Δσ
1.833	0.66	0.10	0.12	0.05	2.92	0.20	0.049	0.028
1.916	0.80	0.11	0.27	0.05	2.39	0.08	0.034	0.020
1.952					1.51	0.54		
1.968					1.51	0.45		
1.980					1.53	0.19		
1.983	0.17	0.11						
1.996			0.43	0.15			-0.034	0.086
1.998					1.26	0.20		
2.013	0.33	0.07						
2.021					1.06	0.24		
2.029			0.38	0.10			0.086	0.07
2.046			0.26	0.12			0.15	0.06
2.048	0.23	0.05						
2.050					1.17	0.21		
2.055					1.15	0.26		
2.062			0.45	0.10			0.18	0.06
2.076					0.98	0.18		
2.080			0.61	0.18			0.17	0.09
2.090							0.25	0.13
2.096					0.95	0.37		
2.108			0.37	0.15			0.31	0.07
2.109	0.48	0.11						
2.111					1.11	0.15		
2.130							0.63	0.14
2.135					0.85	0.24		
2.144							0.61	0.13
2.146					1.12	0.16		
2.154			0.71	0.28			0.91	0.18
2.157	0.75	0.10						
2.165							0.96	0.30
2.175							0.85	0.23
2.182	1.09	0.53	0.46	0.34	1.41	0.60	1.17	0.35
2.197	1.03	0.46					1.29	0.30
2.213							1.22	0.28
2.221	1.69	0.35						
2.235							1.72	0.29
2.254							1.43	0.30
2.335	3.09	0.19	1.28	0.13	0.95	0.14	3.41	0.15
2.410	3.57	0.08	1.27	0.07	1.09	0.10	4.14	0.15
2.471	4.00	0.30	1.43	0.16	1.15	0.23	4.82	0.23
2.497	4.35	0.20	1.53	0.17	1.03	0.22	4.67	0.16
2.540	5.07	0.15	1.07	0.06	0.82	0.15	4.85	0.10
2.569	5.09	0.70	1.24	0.31	1.00	0.30	5.45	0.20
2.602	5.49	0.24	1.03	0.07	0.84	0.23	5.03	0.11
2.603	5.95	0.49	1.42	0.23	0.73	0.25	4.87	0.30
2.623	5.88	0.56	1.16	0.19			4.93	0.24
2.661	5.76	0.64	1.28	0.32			5.54	0.52
2.707	5.43	0.41	1.15	0.12	0.72	0.30	4.97	0.17
2.728	6.05	0.65	1.14	0.13			5.34	0.27
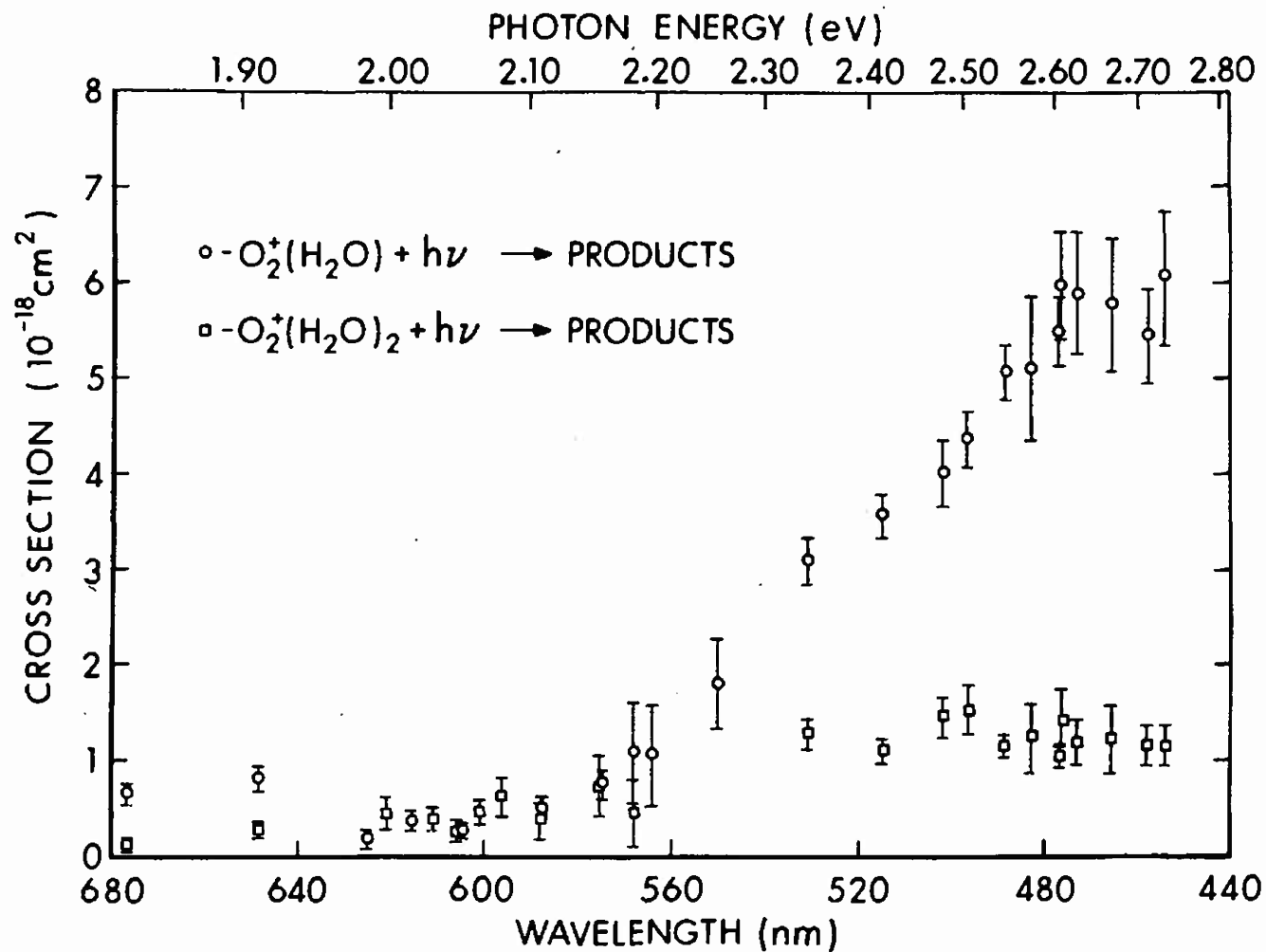
Figure 4. Photodissociation cross section versus photon energy for $O_2^+(H_2O)$ and $O_2^+(H_2O)_2$. The open circles represent the data for $O_2^+(H_2O)$ and the open squares that for $O_2^+(H_2O)_2$.
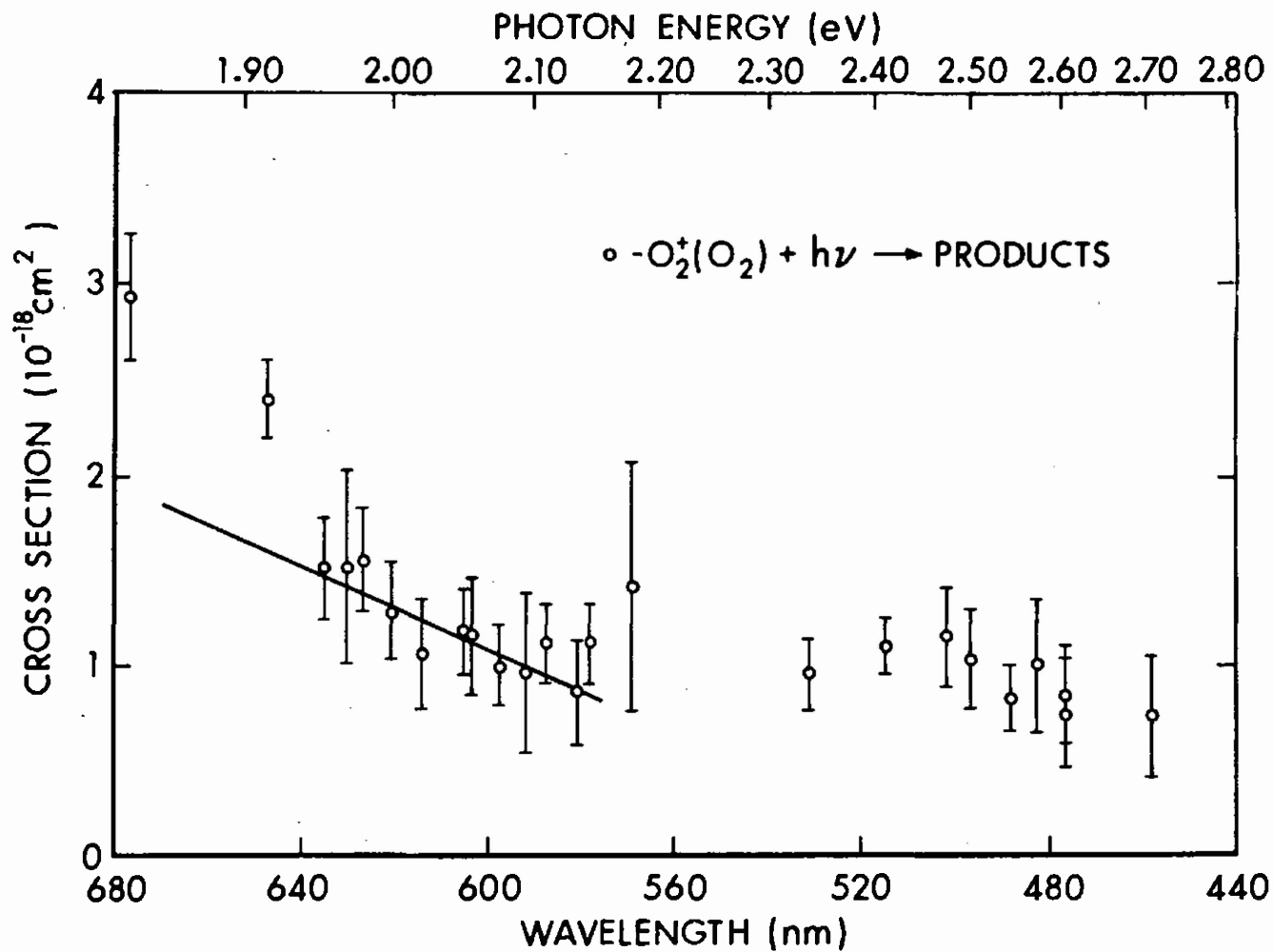
Figure 5. Photodissociation cross section data versus photon energy for $O_2^+(O_2)$. The solid line represents relative photodissociation data for $O_2^+(O_2)$ obtained by Cosby[2].

Measurements have not been reported for the mobility of $O_2^+(H_2O)$ in O_2. This mobility was calculated by mass scaling to the measured mobility of O_3^- in O_2, the resultant value being 2.51×10^{-4} m^2/V-s.

A number of experimental parameters have been varied in an effort to verify that the measured cross sections are characteristic of a single photon process with thermalized ions. The O_2 pressure has been varied from 16 to 40 N/m^2 and the drift distance varied from 37.6 to 112.8 mm. Changing the pressure and drift distance varies the number of low energy collisions made by the ions; hence, a cross section that is independent of these parameters should be characteristic of thermal ions. With the above variations, the cross section of $O_2^+(H_2O)$ at 514.5 nm (one of the most intense laser lines) showed no variation greater than one standard deviation from counting statistics. The intensity of the laser has also been changed over a factor of two without changing the value of the measured cross section of $O_2^+(H_2O)$ at 514.5 nm. This result indicates that the measured photodissociation is a single photon process. One could also conclude that there is no strong laser power dependence in the cross sections of these ions due to the smoothness of the measured curve in the presence of substantial changes in photon flux with wavelength of the laser.

A parameter that did influence the measured photodissociation cross section values was the position of the laser beam relative to the sampling orifice. Three different lasers, an argon ion, a krypton ion, and a tunable dye laser, are used in this experimental set up; hence, the alignment is not necessarily the same for each laser. Without careful alignment it was found that the measured cross section of $O_2^+(H_2O)$ varied as much as 30 per cent between the argon line at 476.5 nm and the krypton line at 476.2 nm. By positioning the laser beams as close as possible to the sampling orifice, i.e., with the edge of the laser beam on the plate containing the orifice, the data obtained became consistent. An explanation for this geometric dependence is recombination effects. That is, photofragments may recombine to form again the ion under study in the distance between the beam and the sampling exit. As the distance to the sampling orifice is decreased for the photofragments there is

27

less time for this effect to occur. In the configuration used for data acquisition no significant error should be present from this effect.

The 22 points displayed for $O_2^+(H_2O)$ in Figure 4 and the 24 shown for $O_2^+(O_2)$ in Figure 5 indicate that both of these cross sections are smooth functions of photon energy over the range reported here. For the case of $O_2^+(O_2)$ there are other experimental data for comparison. The straight line drawn on Figure 5 represents the relative photodissociation cross section data furnished by Cosby.[2] This line is an extrapolation of data points taken at about 0.0002 eV intervals with a resolution of about 10^{-4} eV. These data are in good agreement with our tunable dye laser results displayed as the points covering the range from 577.6 to 635.0 nm. The two krypton lines at 676.4 and 647.1 nm appear to give larger cross section values than the dye laser results would indicate, the 647.1 nm value being about 50 per cent larger than the data of Cosby.

It is observed that the $O_2^+(H_2O)$ cross section is increasing over the photon energy range (2.2-2.7 eV), while the $O_2^+(O_2)$ cross section remains essentially constant over the same range. One may therefore conclude that the photon absorption mechanism is not likely to result from a vibrational transition of O_2^+. Moreover, since O_2 is a homonuclear diatomic molecule, it should have no vibrational transitions of sufficient strength to account for a cross section of the observed magnitude. Since the only exothermic photodestruction reaction for this cluster at the photon energies used here is

$$O_2^+(O_2) + h\nu \longrightarrow O_2^+ + O_2 \qquad\qquad \text{IV}$$
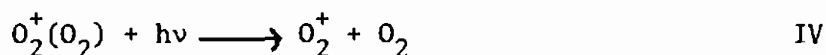
the photon absorption is thought to be due to a transition to an $O_2^+ - O_2$ repulsive state with the observed shape of the cross section due to the relative shapes of the bound and repulsive potential curves. The observed cross section may be considered to be part of a photodissociation curve from one vibrational level such as discussed by von Busch and Dunn[23] in the case of H_2^+.

[23]F. von Busch and G. H. Dunn, Phys. Rev. 5, 1726 (1972).

In the case of $O_2^+(H_2O)$ the simplest photodissociation reaction which is highly exothermic is

$$O_2^+(H_2O) + h\nu \longrightarrow O_2^+ + H_2O \qquad \qquad V$$
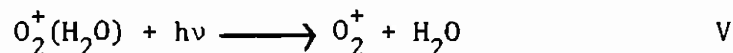
where the bond energy of $O_2^+(H_2O)$ is about 0.8 eV,[24] much less than the incident photon energy. Another possible photodissociation reaction that becomes exothermic at photon energies above about 1.4 eV is

$$O_2^+(H_2O) + h\nu \longrightarrow H_2O^+ + O_2 \qquad \qquad VI$$
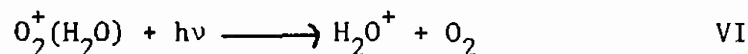
To investigate the possible existence of reaction VI we looked for the appearance of the H_2O^+ photofragment with photons of energy 2.603 eV but no H_2O^+ was detected. However, this result is not conclusive since the charge transfer reaction

$$H_2O^+ + O_2 \longrightarrow O_2^+ + H_2O \qquad \qquad VII$$
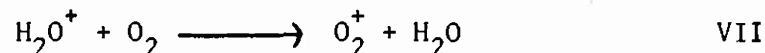
may occur prior to sampling. Taking the rate coefficient for reaction VII as 2×10^{-10} cm^3/s,[25] and using our typical oxygen pressure, a mean lifetime is computed to be about 10^{-7}s, a time short compared with the 10^{-5}s it takes an H_2O^+ ion to traverse the laser beam.

Geometrical considerations may also play a role in the detection of photofragment ions. Due to the position of the Brewster windows on the laser tube and drift tube system the light polarization is fixed in the vertical plane. This can lead to an orientation dependence for photon absorption. Some orientations may diminish the sampling efficiency, e.g., the photofragments being ejected perpendicular to the sampling orifice.

[24]F. C. Fehsenfeld, M. Mosesman, and E. E. Ferguson, J. Chem. Phys. 55, 2115 (1971).

[25]F. C. Fehsenfeld, E. E. Ferguson, A. L. Schmeltekopf, J. Chem. Phys. 46, 2802 (1967).

For neither the $O_2^+(H_2O)$ or $O_2^+(O_2)$ ions were we able to study production of O_2^+ photofragments. O_2^+ is the dominant ion to the extent that O_2^+ photofragments would be less than statistical counting noise for reasonable experimental times. Because of the similarity of the mobilities of the ions involved, we were also unable to separate O_2^+ photofragments from other O_2^+ ions on the basis of time arrival spectra. Whether reaction V or VI is the correct interpretation for the observed photodissociation, it is apparently due to an electronic transition to a repulsive state of either O_2^+ - H_2O or O_2 - H_2O^+.

C. $H^+(H_2O)_n$, n = 1 - 4

The earlier results of Henderson and Schmeltekopf[4] set upper limits on the cross section for photodissociation of hydrated protons in the wavelength region from 580 to 610 nm. Since our apparatus can be varied over a much greater wavelength region by using the discrete ion laser lines, we extended measurements of the photodissociation cross sections of these ions which are dominant positive ions in the D region of the atmosphere. These measurements were conducted at a total pressure of 32.0 N/m^2 (240 mTorr) of oxygen and water vapor, of which approximately 1.3 N/m^2 was water vapor. Measurements were normalized to the photo-detachment cross section of O_2^-.

No evidence for any photodissociation was found at any of the seven wavelengths where measurements were made. Although the cross section of an ion $H^+(H_2O)_n$ could be underestimated by photofragments from $H^+(H_2O)_{n+1}$, measurements made under varying experimental conditions which changed the relative ion densities showed no photodissociation cross sections for any of these ions. From our observations, upper limit estimates have been made of the cross sections for photodissociation of these ions. The values given in Table III are dominated by the uncertainty involved in counting, including possible error limits in the O_2^- cross section, mobility values, drift field, pressure, and laser power as discussed in the errors section. Although each ion was studied individually, the cross section limits are listed together for each wavelength since the upper bounds are similar; the true photodissociation cross sections may

Table III. Photodissociation Cross Section Upper Limits for $H^+(H_2O)_{n=1-4}$ at an E/N = 14.3 Td

Energy (eV)	$\sigma_{H^+(H_2O)}$ (10^{-22} m^2)	$\sigma_{H^+(H_2O)_2}$ (10^{-22} m^2)	$\sigma_{H^+(H_2O)_3}$ (10^{-22} m^2)	$\sigma_{H^+(H_2O)_4}$ (10^{-22} m^2)
1.833	0.17	0.11	0.14	0.07
1.916	0.04	0.05	0.04	0.04
2.410	0.18	0.18	0.16	0.13
2.497	0.36	0.25	0.43	0.24
2.540	0.13	0.08	0.19	0.07
2.602	0.60	0.23	0.24	0.29
2.707	0.85	0.52	0.69	0.97

well be much smaller than these values, or zero. Our limits agree with the earlier ones of Henderson and Schmeltekopf and extend the region of measurements across most of the visible spectrum.

D. $O_2^+(H_2O)_2$ and $O_2^+(CO_2)$

Studies were also made using a gas mixture of 1.33 N/m^2 (10 mTorr) oxygen, 30.7 N/m^2 (230 mTorr) carbon dioxide, and a trace of water. The ions formed in the O_2 -H_2O mixtures discussed in section B were also formed with this mixture, moreover the magnitude of $O_2^+(H_2O)_2$ increased greatly, sufficient for experimental investigation. In addition to these positive ions a large signal for the $O_2^+(CO_2)$ cluster was also present. Photodissociation cross sections as a function of photon energy for the $O_2^+(H_2O)_2$ and $O_2^+(CO_2)$ are given on Figures 4 and 6, respectively, and their values listed in Table II. These cross sections were placed on an absolute scale by normalization to O^-. To accomplish this the gas mixture was first pumped out and the drift tube then refilled to the same total pressure with oxygen. Following that the same procedure prescribed in section B was used. Mobilities for $O_2^+(H_2O)_2$ and $O_2^+(CO_2)$ in both CO_2 and O_2 were required. Snuggs et al.[16] have measured the mobility of CO_4^- in O_2 as 2.45 x 10^{-4} m^2/V-s; we assume the same mobility for both $O_2^+(H_2O)_2$ and $O_2^+(CO_2)$ in O_2. To obtain the mobilities of $O_2^+(H_2O)_2$ and $O_2^+(CO_2)$ in CO_2 we mass scaled using the value of 1.95 x 10^{-4} m^2/V-s for O^- in CO_2.[2] The results obtained are 1.27 x 10^{-4} m^2/V-s for $O_2^+(CO_2)$ in CO_2 and 1.29 x 10^{-4} m^2/V-s for $O_2^+(H_2O)_2$ in CO_2. Blanc's law was applied to obtain the appropriate mobilities for the gas mixture.

Over most of the photon energy range studied the photodissociation cross section for $O_2^+(H_2O)_2$ was substantially less than that for $O_2^+(H_2O)$ even though there are more possible exothermic reaction channels. Whether the addition of neutral molecules to an ion cluster in general dilutes the photon absorption strength cannot be conjectured at this time since this measurement represents only one measurement of the photodissociation of a positive ion double cluster.

The photodissociation cross section values of $O_2^+(CO_2)$ are similar to those of $O_2^+(H_2O)$, as can be seen by comparing Figures 4 and 6.
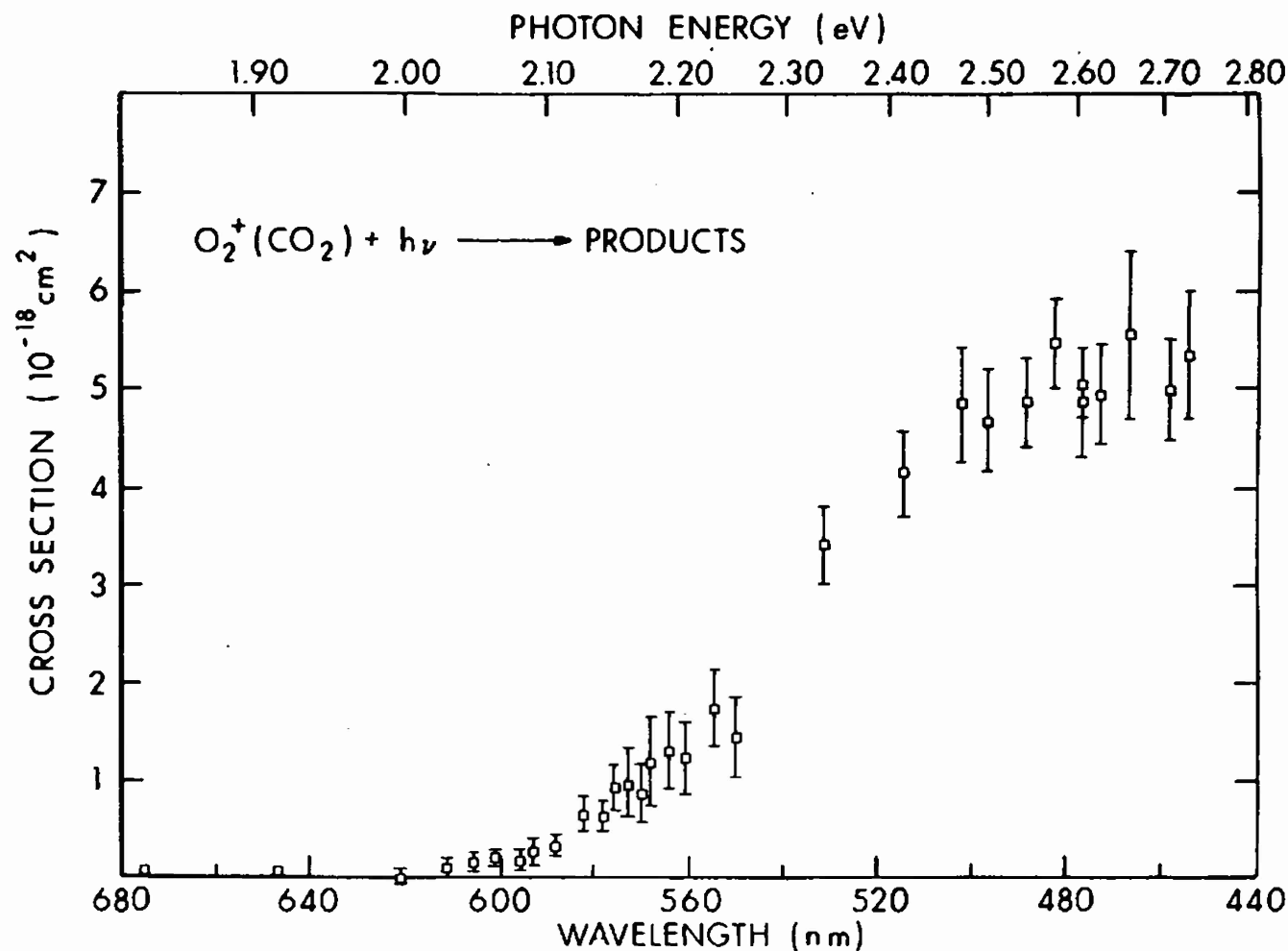
32

Figure 6. Photodissociation cross section data versus photon energy for $O_2^+(CO_2)$. The appearance of a CO_2^+ photofragment at about 2.16 eV indicates that the reaction $O_2^+(CO_2) + h\nu \rightarrow CO_2^+ + O_2$ is occurring.

However, the photodissociation cross section for $O_2^+(CO_2)$, within detection sensitivity, exhibits a threshold in the photon energy region of 2.02 eV, whereas $O_2^+(H_2O)$ does not. The actual threshold may be closer to 2.1 eV since a Maxwellian spread in the energy distribution of $O_2^+(CO_2)$ could account for a low energy tail of $\sim$ 0.1 eV. Exothermic reactions available for photon absorption over the energy range studied here are

$$O_2^+(CO_2) + h\nu \longrightarrow O_2^+ + CO_2 \qquad\qquad \text{VIII}$$
$$\longrightarrow CO_2^+ + O_2 \ . \qquad\qquad \text{IX}$$
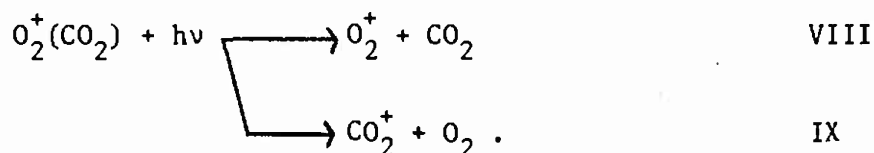
The occurrence of reaction IX was verified by observation of the CO_2^+ photofragment ion. The threshold for the appearance of this photofragment was found to occur at about 2.16 eV indicating that this photon energy absorption is sufficient to place the $O_2^+(CO_2)$ on a $O_2 - CO_2^+$ dissociating curve. With this information an upper limit can be calculated for the dissociation energy of $O_2^+(CO_2)$. That is,

$$D\left[O_2^+(CO_2)\right] \leq 2.16 \text{ eV} - \left[IP(CO_2) - IP(O_2)\right]$$

where IP stands for ionization potential. Using 13.769 eV[26] and 12.063 eV[27] as the ionization potentials of CO_2 and O_2, respectively, an upper limit for the dissociation energy is placed at 0.46 eV.

Spears[28] calculated the binding energies of $Na^+(CO_2)$ and $K^+(CO_2)$ to be 0.544 eV and 0.404 eV, respectively. Considering that these ion clusters should have ion-neutral forces similar to $O_2^+(CO_2)$ these published values indicate that the upper limit on the binding energy obtained for $O_2^+(CO_2)$ is quite reasonable.

The signal strength of O_2^+ here again was too large to determine whether reaction VIII was also contributing to the photodissociation process.

[26]G. Herzberg, *Electronic Spectra and Electronic Structure of Polyatomic Molecules*, Van Nostrand Company, Princeton, New Jersey, 1966.
[27]R. K. Asundi, *Curr. Sci.* **37**, 160 (1968).
[28]K. G. Spears, *J. Chem. Phys.* **57**, 1850 (1972).

At the highest photon energy values studied both the $O_2^+(H_2O)$ and the $O_2^+(CO_2)$ show indications of a plateau. If the interpretation that the photon absorption is due to a transition between a ground vibrational bound state and a repulsive state is valid then one might expect that the photodissociation cross section would decrease due to the symmetric nature of the probability distribution for the ion cluster in its ground vibrational state. However, if another repulsive state is encountered the photodissociation would then again be enhanced.

IV. ERROR ANALYSIS

The uncertainties associated with these measurements may be divided into two categories: relative errors and absolute errors. The relative error consists of statistical counting error, variations in parameters that determine the ion drift velocity (pressure, temperature, and the drift field), and the uncertainty in the relative laser power measurements. Under most experimental conditions the dominant relative error is due to the statistical counting error, taken as $\pm \sqrt{N}$, where N is the number of ions counted. We estimate the error in the ratio of ion velocities due to error in the pressure, temperature, or drift field to be no more than ± 4 per cent. The laser power ratio measurements are uncertain by ± 3 per cent. The root-mean-square of these contributions is ± 5 per cent. The total relative error is this ± 5 per cent combined with the statistical counting error which varies from point to point. Total relative error is displayed as the error bars given in the figures and the statistical uncertainties are listed in the tables.

The absolute error consists of the uncertainty in the photodetachment cross section for O^- or O_2^-, the reference value, and the uncertainty in the ratio of the ion drift velocities in Eq. 4 due to the mobility values used. When these absolute limits are combined with the relative error, discussed above, an estimate of the overall uncertainty in the values quoted is obtained.

Absolute photodetachment cross sections for O^- over the wavelengths of interest have been obtained by Branscomb et al.[7] with an uncertainty of ± 10 per cent. Photodetachment cross section values for O_2^- were obtained with our apparatus and the total error in the cross sections

must be determined point by point. The uncertainty in the ion drift velocity due to the uncertainty in mobility values varies among the ions. Mobility values taken from Snuggs et al.[16] for O^-, O_2^-, CO_2^-, CO_4^-, and $O_2^+(O_2)$ all measured with molecular oxygen as the neutral gas have a ± 4 per cent uncertainty. Mobility values for O^- and CO_3^- in carbon dioxide were obtained from Cosby[2] and have an uncertainty of ± 5 per cent. The mobilities of the ions $O_2^+(CO_2)$, $O_2^+(H_2O)_{1,2}$, and $H^+(H_2O)_n$ were not found in the literature and have been computed by mass scaling, Eq. 6. Barring anomalous effects such as resonance charge transfer or a neutral gas with a large dipole moment, neither of which should be present in these cases, this method of computing mobilities gives quite good results. We conservatively estimate the uncertainty for these cases to be ± 20 per cent. This uncertainty almost encompasses the entire mass range from 16 to 76 amu for mobility values of well behaved ions in oxygen.

In summary, our estimates of the total error limits for the photo-destruction cross sections reported here are as follows. For O_2^- the cross sections are uncertain to ± 12 per cent (the root-mean-square of relative and absolute uncertainty) plus the contribution from counting, combined in a root-mean-square sense. For CO_3^-, the error limits are ± 7 per cent plus counting and the uncertainty in the O_2^- cross section which must be done point by point. For $O_2^+(O_2)$ our estimate of the error limits is ± 12 per cent plus the counting uncertainty. For $O_2^+(H_2O)_{1,2}$ and $O_2^+(CO_2)$ the total error limits are ± 23 per cent plus the counting error. In setting the upper limits for the photodissociation cross sections for $H^+(H_2O)_{n=1-4}$, the error limits were ± 23 per cent plus the uncertainty in the counting and the O_2^- photodetachment cross section which varies with wavelength.

V. SUMMARY

Upper limits for the absolute photodissociation cross sections have been experimentally determined for thermal positive ion clusters that dominate the D region of the atmosphere, $H^+(H_2O)_{n=1-4}$. The photodissociation cross sections for these ions, as determined with discrete photon energies in the range of 1.83 to 2.71 eV, were found to be small or zero.

36

Other weakly bound positive ion clusters studied that can be present in the atmosphere are $O_2^+(H_2O)_{1,2}$ and $O_2^+(CO_2)$. These ions were studied over the energy range of 1.83 to 2.73 eV. Photodissociation cross sections were found to be sizeable, approaching 6 x 10^{-18} cm^2 at 2.6 eV. A photo-fragment CO_2^+ ion was observed as a consequence of the dissociation of $O_2^+(CO_2)$. From the appearance of this photofragment an upper limit of 0.46 eV was placed on the binding energy of this cluster. More importantly the existence of a photon assisted charge transfer reaction of a type that can be operable in the atmosphere has been observed.

Finding that positive ion clusters can readily dissociate and charge transfer under the influence of visible light requires that charged particle models of the daytime atmosphere consider these processes.

ACKNOWLEDGMENTS

REFERENCES

1. T. M. Miller, J. L. Heidrich, and J. T. Moseley, IX Int. Conf. on the Phys. of Electronic and Atomic Collisions, July 1975.

2. P. C. Cosby, Private Communication (1975).

3. J. A. Vanderhoff and R. A. Beyer, Chem Phys Lett 38, 532 (1976).

4. W. R. Henderson and A. L. Schmeltekopf, J. Chem. Phys. 57, 4502 (1972).

5. T. M. Miller, J. H. Ling, R. P. Saxon, and J. T. Moseley, Phys Rev, to be published.

6. E. E. Ferguson, Rev. Geophys. and Space Phys. 9, 93 (1972).

7. L. M. Branscomb, S. J. Smith, and G. Tisone, J. Chem. Phys. 43, 2906 (1965).

8. E. W. McDaniel and E. A. Mason, The Mobility and Diffusion of Ions in Gases, (John Wiley and Sons, New York, 1973).

9. P. C. Cosby, R. A. Bennett, J. R. Peterson, and J. T. Moseley, J. Chem. Phys., 63, 1612 (1975).

10. P. H. Krupenie, J. Phys. Chem. Ref. Data, 1, 520 (1972).

11. D. S. Burch, S. J. Smith, and L. M. Branscomb, Phys. Rev. 112, 171 (1958).

12. P. Warneck, GCA Technical Report 69-13-N, GCA Corporation, Bedford, MA, 1969.

13. J. A. Burt, Can. J. Phys. 50, 2410 (1972).

14. J. T. Moseley, R. A. Bennett, and J. R. Peterson, Chem. Phys. Lett. 26, 288 (1974).

15. J. T. Moseley, P. C. Cosby, R. A. Bennett, and J. R. Peterson, J. Chem. Phys., 62, 4826 (1975).

16. R. M. Snuggs, D. J. Volz, J. H. Schummers, D. W. Martin, and E. W. McDaniel, Phys. Rev. A 3, 477 (1971).

17. J. A. Burt, J. Chem. Phys. 57, 4649 (1972).

18. E. E. Ferguson, F. C. Fehsenfeld, and A. V. Phelps, J. Chem. Phys. 59, 1565 (1973).

19. J. A. Burt, J. Chem. Phys. 59, 1567 (1973).

REFERENCES (Cont'd)

20. S. P. Hong, S. B. Woo and E. M. Helmy, Bull. Am. Phys. 21, 170 (1976).

21. P. C. Cosby and J. T. Moseley, Phys. Rev. Letters 34, 1603 (1975).

22. C. J. Howard, V. M. Bierbaum, H. W. Rundle, and F. Kaufman, J. Chem. Phys. 57, 3491 (1972).

23. F. von Busch and G. H. Dunn, Phys. Rev. 5, 1726 (1972).

24. F. C. Fehsenfeld, M. Mosesman, and E. E. Ferguson, J. Chem. Phys. 55, 2115 (1971).

25. F. C. Fehsenfeld, E. E. Ferguson, A. L. Schmeltekopf, J. Chem. Phys. 46, 2802 (1967).

26. G. Herzberg, Electronic Spectra and Electronic Structure of Polyatomic Molecules, Van Nostrand Company, Princeton, New Jersey, 1966.

27. R. K. Asundi, Curr. Sci. 37, 160 (1968).

28. K. G. Spears, J. Chem. Phys. 57, 1850 (1972).

This page Left Intentionally Blank

DISTRIBUTION LIST

No. of Copies	Organization	No. of Copies	Organization

12   Commander
Defense Documentation Center
ATTN: DDC-TCA
Cameron Station
Alexandria, VA 22314

1   Director
Institute for Defense Analysis
ATTN: Dr. E. Bauer
400 Army-Navy Drive
Arlington, VA 22202

2   Director
Defense Advanced Research
   Projects Agency
ATTN: STO, CPT J. Justice
       LTC W. A. Whitaker
1400 Wilson Boulevard
Arlington, VA 22209

1   Director of Defense
   Research & Engineering
ATTN: CPT K. W. Ruggles
Washington, DC 20305

4   Director
Defense Nuclear Agency
ATTN: STAP (APTL)
       STRA (RAAE)
         Dr. C. Blank
         Dr. H. Fitz, Jr.
       DDST
Washington, DC 20305

2   DASIAC/DOD Nuclear Information
   and Analysis Center
General Electric Company-TEMPO
ATTN: Mr. A. Feryok
       Mr. W. Knapp
816 State Street
P.O. Drawer QQ
Santa Barbara, CA 93102

1   Director
Defense Communications Agency
ATTN: Code 340, Mr. W. Dix
Washington, DC 20305

1   Commander
US Army Materiel Development
   and Readiness Command
ATTN: DRCDMA-ST
5001 Eisenhower Avenue
Alexandria, VA 22333

1   Commander
US Army Aviation Systems Command
ATTN: DRSAV-E
12th and Spruce Streets
St. Louis, MO 63166

1   Director
US Army Air Mobility Research
   and Development Laboratory
Ames Research Laboratory
Moffett Field, CA 94035

1   Commander
US Army Electronics Command
ATTN: DRSEL-RD
Fort Monmouth, NJ 07703

2   Commander/Director
Atmospheric Sciences Laboratory
US Army Electronics Command
ATTN: Dr. E. H. Holt
       Mr. H. Ballard
White Sands Missile Range
NM 88002

1   Commander
US Army Missile Command
ATTN: DRSMI-R
Redstone Arsenal, AL 35809

41

DISTRIBUTION LIST

No. of Copies	Organization
1	Commander US Army Tank Automotive Development Command ATTN: DRDTA-RWL Warren, MI 48090
2	Commander US Army Mobility Equipment Research & Development Command ATTN: Tech Docu Cen, Bldg 315 DRSME-RZT Fort Belvoir, VA 22060
1	Commander US Army Armament Command Rock Island, IL 61202
2	Commander US Army Harry Diamond Labs ATTN: DRXDO-TI DRXDO-NP Mr. F. Wimenitz 2800 Powder Mill Road Adelphi, MD 20783
1	Director US Army TRADOC Systems Analysis Agency ATTN: ATAA-SA White Sands Missile Range NM 88002
1	Commander US Army Nuclear Agency ATTN: Mr. J. Berberet Fort Bliss, TX 79916
1	Commander US Army Research Office ATTN: Dr. R. Lontz P.O. Box 12211 Research Triangle Park NC 27709

No. of Copies	Organization
2	Commander US Army BMD Systems Command ATTN: SSC-HS, Mr. H. Porter SSC-TET, Mr. E. Carr P.O. Box 1500 Huntsville, AL 35807
1	HQDA (DACS-BMT) Arlington, VA 22209
1	HQDA (DAEN-RDM/Dr. de Percin) Washington, DC 20314
1	Chief of Naval Research ATTN: Code 418, Dr. J. Dardis Department of the Navy Washington, DC 20360
1	Commander US Naval Electronics Laboratory ATTN: Mr. W. Moler San Diego, CA 92152
1	Commander US Naval Surface Weapons Center ATTN: Dr. L. Rutland Silver Spring, MD 20910
3	Director US Naval Research Laboratory ATTN: Dr. W. Ali Code 7700, Mr. J. Brown Code 2020, Tech Lib Washington, DC 20330
3	HQ USAF (AFNIN; AFRD; AFRDQ) Washington, DC 20330
7	AFGL (LKD, Dr. R. Narcisi; LKB, Dr. K. Champion Dr. T. Keneshea Dr. J. Paulson Dr. W. Swider; OPR, Dr. Murphey Dr. Kennelly Hanscom AFB, MA 01731

DISTRIBUTION LIST

No. of Copies	Organization
2	AFSC (DLCAW, LTC R. Linkous; SCS) Andrews AFB Washington, DC 20334
1	Director National Oceanic and Atmospheric Administration ATTN: Dr. E. Ferguson US Department of Commerce Boulder, CO 80302
1	Director Brookhaven National Laboratory ATTN: Docu Sec 25 Brookhaven Avenue Upton, NY 11973
2	Director Los Alamos Scientific Laboratory ATTN: Lib Dr. W. Maier (Gp J-10) P.O. Box 1663 Los Alamos, NM 87544
2	Sandia Laboratories ATTN: Org 3141, Tech Lib Org 100, F. Hudson P.O. Box 5800 Albuquerque, NM 87115
1	Bell Telephone Laboratories, Inc. Technical Report Service ATTN: Tech Rpts Specialist WH 5E-227 Whippany, NJ 07981
1	General Electric Company Valley Forge Space Technology Center ATTN: Dr. M. Bortner P.O. Box 8555 Philadelphia, PA 19101

No. of Copies	Organization
1	Mission Research Corporation ATTN: Dr. M. Schiebe 812 Anacapa Street, Studio 5 Santa Barbara, CA 93101
1	R&D Associates ATTN: Dr. F. Gilmore P.O. Box 9695 Marina del Rey, CA 90291
4	Stanford Research Institute ATTN: Dr. J. Peterson Dr. J. Moseley Dr. P. Cosby Dr. F. Smith 333 Ravenswood Avenue Menlo Park, CA 94025
1	CIRES University of Colorado ATTN: Dr. A. W. Castleman Boulder, CO 80302
1	Georgia Institute of Technology School of Physics ATTN: I. R. Gatland Atlanta, GA 30332
1	Pennsylvania State University Ionospheric Research Laboratory ATTN: Dr. L. C. Hale University Park, PA 16802
1	State University of New York Department of Atmospheric Sciences ATTN: Dr. V. Mohnen Albany, NY 12203
2	University of Colorado Joint Institute for Laboratory Astrophysics ATTN: Dr. W. C. Lineberger Dr. A. V. Phelps Boulder, CO 80304

DISTRIBUTION LIST

No. of
Copies   Organization

1   University of Delaware
     Department of Physics
     ATTN: Prof S. B. Woo
     Newark, DE 19711

1   University of Denver
     Denver Research Institute
     ATTN: Dr. R. Amme
     P.O. Box 10127
     Denver, CO 82010

1   University of Illinois
     Electrical Engineering Department
     Aeronomy Laboratory
     ATTN: Prof C. Sechrist
     Urbana, IL 61801

1   University of Minnesota, Morris
     Division of Science and Mathematics
     ATTN: Dr. M. N. Hirsh
     Morris, MN 56267

1   University of Pittsburgh
     Cathedral of Learning
     ATTN: Dr. M. A. Biondi
     400 Bellefield Avenue
     Pittsburgh, PA 15213

1   University of Texas at El Paso
     Physics Department
     ATTN: J. Collins
     El Paso, TX 70007

Aberdeen Proving Ground

     Marine Corps Ln Ofc
     Dir, USAMSAA